J|A|C|S
ARTICLES

Published on Web 02/25/2009

Chlorination: A General Route toward Electron Transport in Organic Semiconductors

Ming Lee Tang,[†] Joon Hak Oh,[‡] Anna Devi Reichardt,[†] and Zhenan Bao*[,‡]

Departments of Chemistry and Chemical Engineering, Stanford University, Stanford, California 94305

Received November 18, 2008; E-mail: zbao@stanford.edu

Abstract: We show that adding chlorine atoms to conjugated cores is a general, effective route toward the design of n-type air-stable organic semiconductors. We find this to be true for acenes, phthalocyanines, and perylene tetracarboxylic diimide (PDI)-based molecules. This general finding opens new avenues in the design and synthesis of organic semiconductors. We compared a series of fluoro- and chloro-functionalized acenes, phthalocyanines, and PDI-based molecules. The acenes synthesized showed high and balanced ambipolar transport in the top-contact organic field effect transistor (OFET) geometry. The electron-withdrawing halogen groups lowered the LUMO and the charge injection barrier for electrons, such that electron and hole transport occurred simultaneously. If the chlorine added does not distort the planarity of the conjugated core, we found that the chloro-functionalized molecules tend to have a slightly smaller HOMO−LUMO gap and a lower LUMO level than the fluoro-containing molecules, both from calculations and cyclic voltammetry measurements in solution. This is most likely due to the fact that Cl contains empty 3d orbitals that can accept π-electrons from the conjugated core, while F does not have energetically accessible empty orbitals for such delocalization.

Introduction

Organic semiconductors (OSCs) can be chemically tuned to give desired electronic and processing characteristics as the active material in low-cost, large area electronics. For example, materials for organic photovoltaics[1−3] (OPVs) need to absorb as much of the solar spectrum as possible, while organic light-emitting diodes[4−8] (OLEDs) are designed to have efficient fluorescence or phosphorescence. With regards to organic field effect transistors[9] (OFETs), many soluble molecules and polymers with high mobility have been demonstrated,[9,10] shedding light on important structure−property relationships. Indeed, the field is burgeoning with descriptions of hole transporting materials, the majority of OFET materials today. In contrast, there is a glaring lack of electron-transporting n-type organic semiconductors.[11−13]

Electron-transporting OFETs are important for the implementation of complementary circuits, which have low power consumption, high operating speeds and an increased device lifetime. Furthermore n-type and ambipolar[12] materials allow organic light-emitting transistors[12] (OLETs) to be fabricated. OLETs are novel devices that combine the functions of OFETs and OLEDs. Typically, n-type materials are made by attaching strong electron-withdrawing groups such as F,[14] CN,[15] alkanoyl,[16] perfluorobenzene,[17] etc., to the conjugated core to lower the molecular orbital (MO) energy levels, or by functionalizing a conjugated core which is already low in reduction potential, such as buckyballs,[10] naphthalenetetracarboxylic diimide[18,19] (NDI), and perylene tetracarboxylic diimide[20] (PDI)-based molecules. The decreased lowest unoccupied molecular orbital (LUMO) allows electron injection by lowering the charge

[†] Department of Chemistry.
[‡] Chemical Engineering.

(1) Gunes, S.; Neugebauer, H.; Sariciftci, N. S. *Chem. Rev.* **2007**, *107*, 1324–1338.
(2) Blom, P. W. M.; Mihailetchi, V. D.; Koster, L. J. A.; Markov, D. E. *Adv. Mater.* **2007**, *19*, 1551–1566.
(3) Sun, S.-S.; Sariciftci, N. S. *Organic Photovoltaics: Mechanisms, Materials, and Devices*; CRC: Boca Raton, FL, 2005.
(4) Walzer, K.; Maennig, B.; Pfeiffer, M.; Leo, K. *Chem. Rev.* **2007**, *107*, 1233–1271.
(5) Shirota, Y.; Kageyama, H. *Chem. Rev.* **2007**, *107*, 953–1010.
(6) Yang, Y.; Pei, Q.; Heeger, A. J. *J. Appl. Phys.* **1996**, *79*, 934–939.
(7) Friend, R. H.; Gymer, R. W.; Holmes, A. B.; Burroughes, J. H.; Marks, R. N.; Taliani, C.; Bradley, D. D. C.; Dos Santos, D. A.; Bredas, J. L.; Logdlund, M.; Salaneck, W. R. *Nature* **1999**, *397*, 121–128.
(8) Kalinowski, J. *Organic Light-Emitting Diodes: Principles, Characteristics and Processes (Optical Engineering)*; CRC: Boca Raton, FL, 2004.
(9) Bao, Z.; Locklin, J., Eds. *Organic Field-Effect Transistors*, 1st ed.; Optical Science and Engineering Series; CRC Press: Boca Raton, FL, 2007.
(10) Murphy, A. R.; Frechet, J. M. J. *Chem. Rev.* **2007**, *107*, 1066–1096.
(11) Newman, C. R.; Frisbie, C. D.; da Silva, D. A.; Bredas, J. L.; Ewbank, P. C.; Mann, K. R. *Chem. Mater.* **2004**, *16*, 4436–4451.
(12) Zaumseil, J.; Sirringhaus, H. *Chem. Rev.* **2007**, *107*, 1296–1323.
(13) Facchetti, A. *Mater. Today* **2007**, *10*, 28–37.
(14) Schmidt, R.; Ling, M. M.; Oh, J. H.; Winkler, M.; Konemann, M.; Bao, Z. N.; Wurthner, F. *Adv. Mater.* **2007**, *19*, 3692–3695.
(15) Jones, B. A.; Ahrens, M. J.; Yoon, M. H.; Facchetti, A.; Marks, T. J.; Wasielewski, M. R. *Angew. Chem., Int. Ed.* **2004**, *43*, 6363–6366.
(16) Yoon, M. H.; DiBenedetto, S. A.; Facchetti, A.; Marks, T. J. *J. Am. Chem. Soc.* **2005**, *127*, 1348–1349.
(17) Yoon, M. H.; Facchetti, A.; Stern, C. E.; Marks, T. J. *J. Am. Chem. Soc.* **2006**, *128*, 5792–5801.
(18) Katz, H. E.; Lovinger, A. J.; Johnson, J.; Kloc, C.; Siegrist, T.; Li, W.; Lin, Y. Y.; Dodabalapur, A. *Nature* **2000**, *404*, 478–481.
(19) See, K. C.; Landis, C.; Sarjeant, A.; Katz, H. E. *Chem. Mater.* **2008**, *20*, 3609–3616.
(20) Horowitz, G.; Kouki, F.; Spearman, P.; Fichou, D.; Nogues, C.; Pan, X.; Garnier, F. *Adv. Mater.* **1996**, *8*, 242–245.

injection barrier. Additionally, a lower LUMO makes the electrons in the LUMOs less susceptible to ambient oxidation. For example, Jones and co-workers report that if the LUMO is below −4.3 eV[21] for PDI and NDI molecules, air-stable n-type OFET operation is observed.

In this paper, we show that Cl can also be used to lower MO energies effectively. Even though Cl is less electronegative than F (Pauline electronegativity[22] for Cl: 3.16; for F: 3.98), we found that molecules functionalized with Cl perform as well as their F-containing counterparts, both in terms of OFET electron mobility and ambient stability. Conjugated cores substituted with Cl typically showed a lower HOMO−LUMO gap than the F counterparts (as inferred by the red-shift of the absorption edge and the λ_{MAX} of the longest wavelength absorption peak in UV−vis) provided no significant steric hindrance is introduced that twists the conjugated core. In addition, the LUMO of the Cl substituted molecule tends to be lower than that of the F substituted one. By making a series of molecules in the acene family and supporting our experimental data with density functional theory (DFT) calculations, this trend is seen not only for acenes, but also for **F_{16}CuPc** and **Cl_{16}CuPc**,[23] as well as PDI-based molecules.[24,25] The synthetic accessibility and lower cost of chloro-containing precursors makes this observation acutely significant. Thus we present a new, general design rule toward n-type OSCs.

Experimental Methods

Instrumentation. NMR (^{1}H and ^{13}C) spectra were recorded on a Varian Inova−500 MHz spectrometer at room temperature unless indicated otherwise. The ^{1}H and ^{13}C Chemical shifts (δ) are reported in parts per million and the residual solvent peak was used as an internal standard. The Philips PANalytical X'Pert diffractometer with a PreFIX X-ray mirror at the incident beam, and a parallel plate collimator at the diffracted beam was used on the thin films of the evaporated molecules. $\omega/2\theta$ scans were performed with Cu Kα radiation at a power of 45 mV and 40 mA, with a step size of 0.02°, and a step time of 1.0 s. A Digital Instruments (DI) MMAFM-2 scanning probe microscope was used to perform tapping mode AFM on the samples with a silicon tip of 300 kHz frequency. DI Nanoscope software was used to process the raw AFM images. Cyclic voltammetry were recorded on a CHI411 instrument from CH Instruments, Inc. UV−vis was recorded with a Varian Cary 6000i UV−vis spectrophotometer with samples prepared in ambient. Ultraviolet photoelectron spectroscopy (UPS) in ambient was performed with a Riken Keiki Co. Ltd. model AC-2 Surface Analyzer to obtain the ionization potential of the 45 nm organic thin films.

Crystallographic Investigations. Single crystals of the materials were analyzed on a Bruker-Nonius X8 Proteum CCD diffractometer using Cu Kα radiation.

FET Device Fabrication. Top contact devices were made according to a literature procedure.[26] A thermally grown dry silicon dioxide layer (300 nm) with a capacitance per unit area of 1.0×10^{-8} F/cm^2 functioned as the dielectric, while a heavily n-doped silicon substrate functioned as the gate electrode. First, the substrates were cleaned by immersion in freshly prepared piranha solution for 45 min. Octadecyltrimethoxysilane (OTS) treatment was done by spin-coating a 3 mM solution of OTS in trichloroethylene on the piranha-cleaned wafer, then placing the substrate in an environment saturated with ammonia vapor for 12 h, followed by rinsing in toluene. Shadow masks with *W*/*L* of 20 ($W = 1000$ μm, $L = 50$ and $W = 2000$ μm, $L = 100$ μm) were used after the evaporation of the organic semiconductor to deposit the gold drain and source electrodes. The organic semiconductors were deposited at a rate of 0.2−0.3 Å/s under a pressure of $4-6 \times 10^{-6}$ torr to a final thickness of 45 nm as determined in situ by a quartz crystal monitor. TFT measurements were performed in air (the relative humidity ∼45%) or in the nitrogen glovebox using a Keithley 4200 semiconductor parameter analyzer (oxygen levels <1 ppm).

Results

Synthesis. The new asymmetric, tetrachlorinated triisopropylsilyl (TIPS)-acetylene functionalized pentacene and tetraceno[2,3-*b*]thiophene molecules were synthesized as shown in Scheme 1. The details are in the Supporting Information. The synthetic scheme was based on previous work,[27,28] but with a few modifications. First, the Friedel−Crafts acylation of tetrachlorophthalic anhydride, **1**, with hydroquinone was performed in the molten salt of $AlCl_3$ and 1-ethyl-3-methylimidazolium chloride (MeEtImCl),[29] instead of the more conventional $AlCl_3$/NaCl[30] melt. We found that the $AlCl_3$/MeEtImCl melt facilitated reactions on a 5−10 g scale, because the lower viscosity of the reaction mixture allowed stirring after all the reactants were added, in contrast to the $AlCl_3$/NaCl melt where stirring stopped relatively soon.

The tetrachloro-containing precursors were in general more insoluble than their tetrafluoro counterparts. Therefore, no proton NMR of quinones **6** and **7** could be obtained even at high temperature, while both proton and fluorine NMR of the tetrafluorinated quinones could be obtained relatively easily at room temperature. However, once the TIPS-acetylene groups were added, they were all very soluble in common organic solvents. **$TIPSEpentF_4$** and **$TIPSEpentF_8$** (Figure 1) were synthesized according to literature procedures.[27] All the TIPS-acetylene-containing molecules were purified by recrystallization in degassed hexanes two to three times before device fabrication. **Cl_{16}CuPc** was purified by sublimation in high vacuum in a three-zone furnace twice before devices were made at a substrate temperature of 200 °C. The PDI-based molecules are listed in Figure 1 for the purposes of discussion. The results cited here are from previous literature reports.[14,15,20,21,24,31,32]

Various attempts were made, but we could not synthesize the octachloro-containing pentacene molecule, **$TIPSEpentCl_8$** (Figure 1). Efforts to make the 3,4,5,6-tetrachlorobenzene-1,2-dicarbaldehyde for the aldol condensation failed. The Diels−Alder reaction coupling 1,2-bis(bromomethyl)-3,4,5,6-tetrachlorobenzene with **3**, 6,7,8,9-tetrachloro-1,4-anthraquinone, made the desired octachloro-pentacenequinone as determined by mass spectrometry, but reaction with TIPS-acetylide in various solvents did not give the target molecule.

Electronic Structure Characterization. We investigated the energy levels of **$TIPSEthiotetCl_4$**, **$TIPSEpentCl_4$**, **TIP-**

(21) Jones, B. A.; Facchetti, A.; Wasielewski, M. R.; Marks, T. J. *J. Am. Chem. Soc.* **2007**, *129*, 15259–15278.
(22) Allred, A. L. *J. Inorg. Nucl. Chem.* **1961**, *17*, 215.
(23) Ling, M. M.; Bao, Z. N.; Erk, P. *Appl. Phys. Lett.* **2006**, *89*, 163516.
(24) Ling, M. M.; Erk, P.; Gomez, M.; Koenemann, M.; Locklin, J.; Bao, Z. N. *Adv. Mater.* **2007**, *19*, 1123–1127.
(25) Chen, Z. J.; Debije, M. G.; Debaerdemaeker, T.; Osswald, P.; Wurthner, F. *ChemPhysChem* **2004**, *5*, 137–140.
(26) Locklin, J.; Roberts, M. E.; Mannsfeld, S. C. B.; Bao, Z. *J. Macromol. Sci., Part C: Polym. Rev.* **2006**, *46*, 79–101.
(27) Swartz, C. R.; Parkin, S. R.; Bullock, J. E.; Anthony, J. E.; Mayer, A. C.; Malliaras, G. G. *Org. Lett.* **2005**, *7*, 3163–3166.
(28) Tang, M. L.; Reichardt, A. D.; Miyaki, N.; Stoltenberg, R. M.; Bao, Z. *J. Am. Chem. Soc.* **2008**, *130*, 6064–6065.
(29) Boon, J. A.; Levisky, J. A.; Pflug, J. L.; Wilkes, J. S. *J. Org. Chem.* **1986**, *51*, 480–483.
(30) Chen, Z. H.; Swager, T. M. *Org. Lett.* **2007**, *9*, 997–1000.
(31) Debije, M. G.; Chen, Z. J.; Piris, J.; Neder, R. B.; Watson, M. M.; Mullen, K.; Wurthner, F. *J. Mater. Chem.* **2005**, *15*, 1270–1276.
(32) Wurthner, F.; Osswald, P.; Schmidt, R.; Kaiser, T. E.; Mansikkamaki, H.; Konemann, M. *Org. Lett.* **2006**, *8*, 3765–3768.

Scheme 1. Synthesis of Chlorinated TIPS-Acetylene Functionalized Acenes[a]

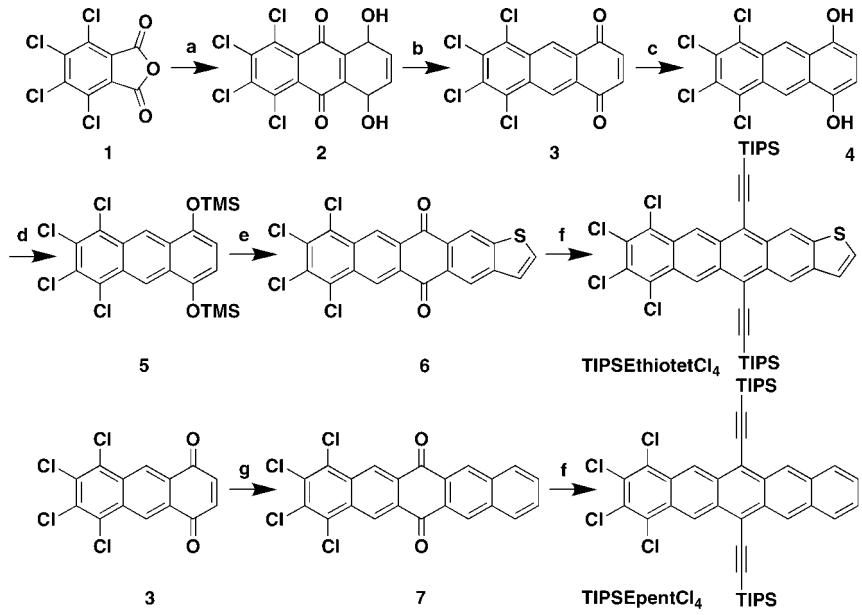

[a] Reagents and conditions: (a) Hydroquinone, $AlCl_3$, MeEtImCl, 180°C; (b) $NaBH_4$, MeOH, reflux; (c) $Na_2S_2O_4$, water, dioxane; (d) TMSCl, HMDS, CH_3CN, RT; (e) i, 2,3-thiophenedicarbaldehyde, tris(pentafluorophenyl)boron, CH_2Cl_2, RT; ii, CF_3CH_2OH, reflux; (f) i, *n*BuLi, ether, TIPSacetylene, 60°C; ii, $SnCl_2 \cdot H_2O$, 60°C; (g) α,α,α′,α′-tetrabromo-*o*-xylene, KI, DMF, 60°C.

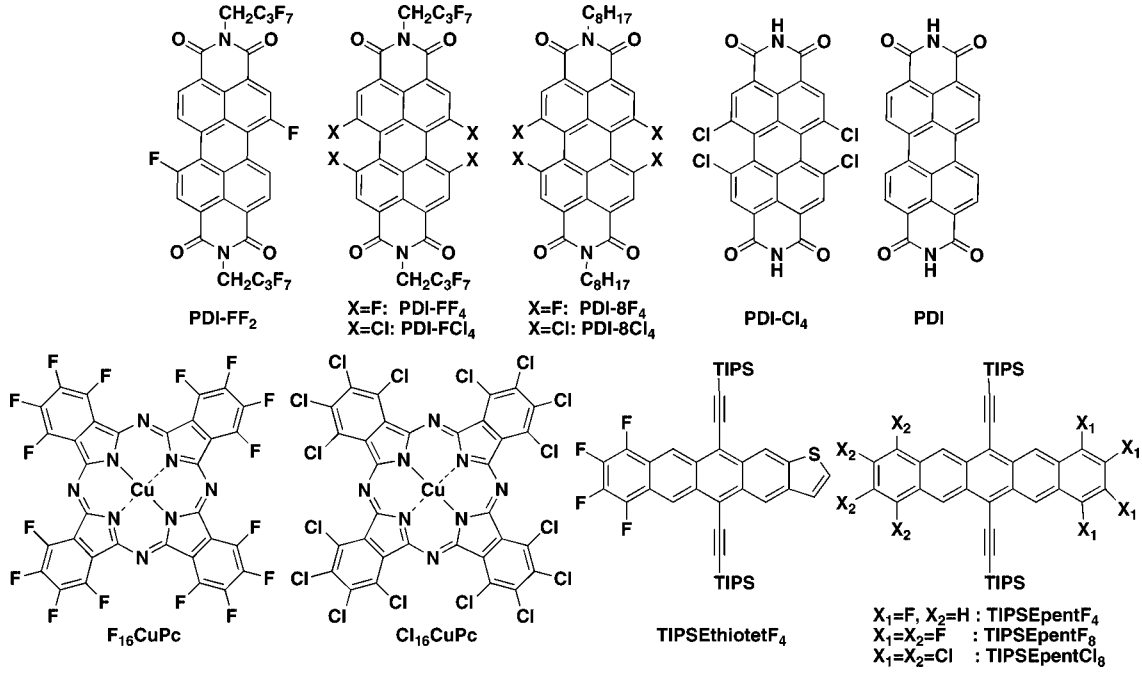

Figure 1. n-Type molecules discussed in this paper. Top row: perylene carboxylic diimide (PDI) derivatives. Bottom row: halogenated copper phthalocyanines (CuPc) and acenes.

SEthiotetF$_4$, **TIPSEpentF$_4$**, and **TIPSEpentF$_8$** both in thin film and in solution. Cyclic voltammetry was carried out to obtain the highest occupied molecular orbital (HOMO) and lowest unoccupied molecular orbital (LUMO) in solution. The thin films made by vacuum thermal evaporation under the same conditions used for device preparation in high vacuum gave us the bandgap (E_g), by UV−vis, and the ionization potential (I), by ultraviolet photoelectron spectroscopy (UPS). Density functional theory calculations were performed with the B3LYP level of theory with a 6-31G+d basis set using the Gaussian03[33] program. The results are summarized in Table 1 and are shown graphically in Figure 2.

As can be seen, the measured and calculated HOMO and LUMO levels share the same trends. The HOMOs of **TIPSEpentF$_4$** and **TIPSEpentCl$_4$** are around −5.35 eV, while those of **TIPSEthiotetF$_4$** and **TIPSEthiotetCl$_4$** are around −5.39 eV. DFT calculations suggest that the pentacene-based molecules have a similar HOMO of −5.09 eV, while the tetraceno[2,3-*b*]thiophene molecules have the same HOMO of −5.17 eV, even though F is more electronegative than Cl. The experimental HOMOs, however, as measured by a pair of reversible oxidation

(33) Frisch, M. J. T.; et al. *Gaussian03*; Gaussian Inc: Wallingford, CT, 2004.

Table 1. Summary of the HOMO−LUMO and λ_{MAX} in Solution; the Workfunction, *I*, and Bandgap, E_g, in Thin Film, As Well As the HOMO−LUMO Levels Predicted by DFT of the Acenes

	solution				thin film[c]		DFT calc[f].	
molecule	λ_{MAX} (nm)[a]	HOMO(eV)[b]	LUMO (eV)[b]	HOMO−LUMO (eV)	*I* (eV)[d]	E_g (eV)[e]	HOMO (eV)	LUMO (eV)
TIPSEthiotetF$_4$	597	−5.39	−3.35	2.04	−5.26	1.82	−5.17	−3.04
TIPSEthiotetCl$_4$	613	−5.38	−3.45	1.93	−5.13	1.73	−5.17	−3.08
TIPSEpentF$_4$	639	−5.35	−3.49	1.86	−5.24	1.66	−5.09	−3.17
TIPSEpentCl$_4$	654	−5.36	−3.55	1.81	−5.13	1.61	−5.09	−3.21
TIPSEpentF$_8$	630	−5.54	−3.60	1.94	−5.59	1.68	−5.45	−3.52
TIPSEpentCl$_8$	–	–	–	–	–	–	−5.43	−3.55
F$_{16}$CuPc	–	–	–	–	−5.53	1.43	–	–
Cl$_{16}$CuPc	–	–	–	–	−5.65	1.48	–	–

[a] λ_{MAX} measured in THF. [b] HOMO−LUMO measured by cyclic voltammetry in degassed CH_2Cl_2 with 0.1 M $TBAFPF_6$ as the electrolyte, with respect to a Fc/Fc^+ reference (−4.8 eV to vacuum) added after each measurement. [c] 45 nm thin film made by evaporation under high vacuum. [d] *I*, the workfunction measured in ambient by UPS. [e] E_g, the bandgap, on quartz with the long wavelength absorption edge. [f] DFT calculations using Gaussian03 with the B3LYP level of theory and 6-31G+d basis set.

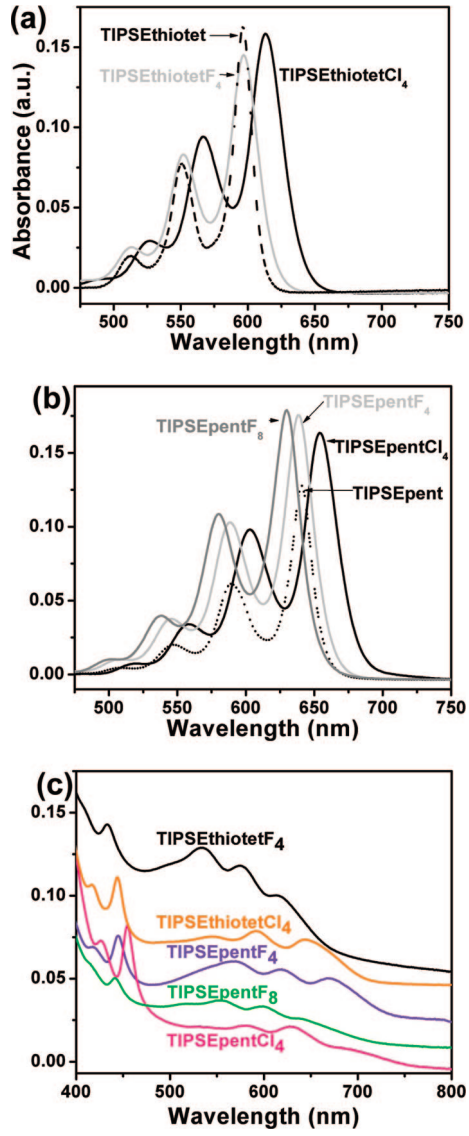

Figure 2. UV−vis of the halogenated acenes. (a) Tetraceno[2,3-*b*]thiophene-based molecules in THF; (b) pentacene-based molecules in THF and (c) 45 nm thin films of the molecules evaporated under device conditions.

and reduction peaks with cyclic voltammetry show that the F substitutions have a HOMO that is 0.01 eV less than the corresponding Cl molecules. Tetrachlorination results in an interesting observation, the LUMO of these molecules is significantly lowered, and a red-shift of 15−16 nm occurs when

Table 2. Summary of the Out-of-Plane XRD Peaks of the Acenes Obtained from 45 nm Thin Films with Cu Kα Radiation at a Power of 45 mV and 40 mA, with a Step Size of 0.02° and a Step Time of 1.0 s

(00*n*)	TIPSEthiotetF$_4$	TIPSEthiotetCl$_4$	TIPSEpentF$_4$	TIPSEpentCl$_4$	TIPSEpentF$_8$
(001)/Å	16.8	17.3	16.7	17.3	16.8
(002)/Å	8.4	8.6	8.4	8.6	8.4
(003)/Å	5.6	5.7	5.6	5.7	5.6
(004)/Å	4.2	4.3	4.2	4.3	4.3
(005)/Å	3.34	3.4	3.4	3.4	3.4

there are four chlorines on the terminal benzene ring, although molecules with four fluorines show no change in their UV−vis absorption compared to their unhalogenated parent molecules. For example, from **TIPSEpentF$_4$** to **TIPSEpentCl$_4$**, the λ_{MAX} in THF shifts from 639 to 654 nm, while from **TIPSEthiotetF$_4$** to **TIPSEthiotetCl$_4$**, the λ_{MAX} shifts from 597 to 613 nm (Table 1 and Figure 2). There is a corresponding decrease in bandgap in thin film (Figure 2c) and in solution (Figure 2a,b) due to a lower LUMO when the molecule is chlorinated.

To find out if core chlorination generally gives lower HOMO−LUMO gaps and lower LUMOs, we compared other commonly known chlorinated molecules with their fluorinated

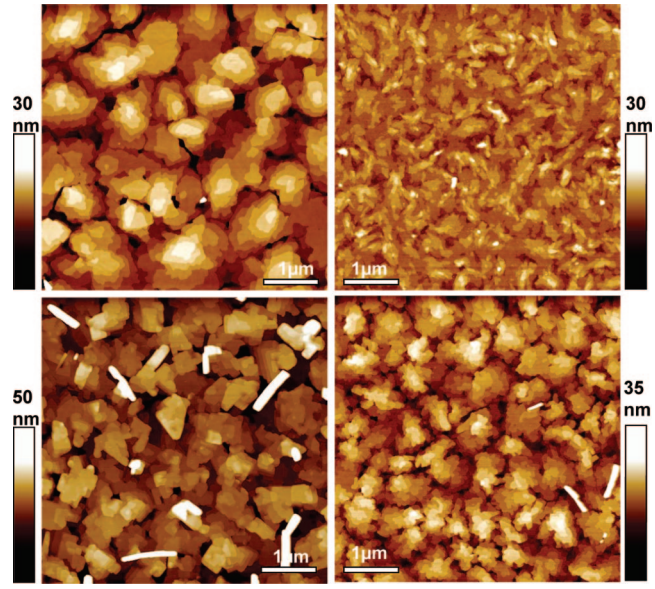

Figure 3. AFM images of the acenes on OTS-treated SiO_2/Si. (Top left) **TIPSEthiotetCl$_4$** at a substrate temperature, T_D = 70 °C. (Top right) **TIPSEpentCl$_4$** at T_D = 60 °C. (Bottom left) **TIPSEpentF$_8$** at T_D = 80 °C. (Bottom right) **TIPSEpentF$_4$** at T_D = RT.

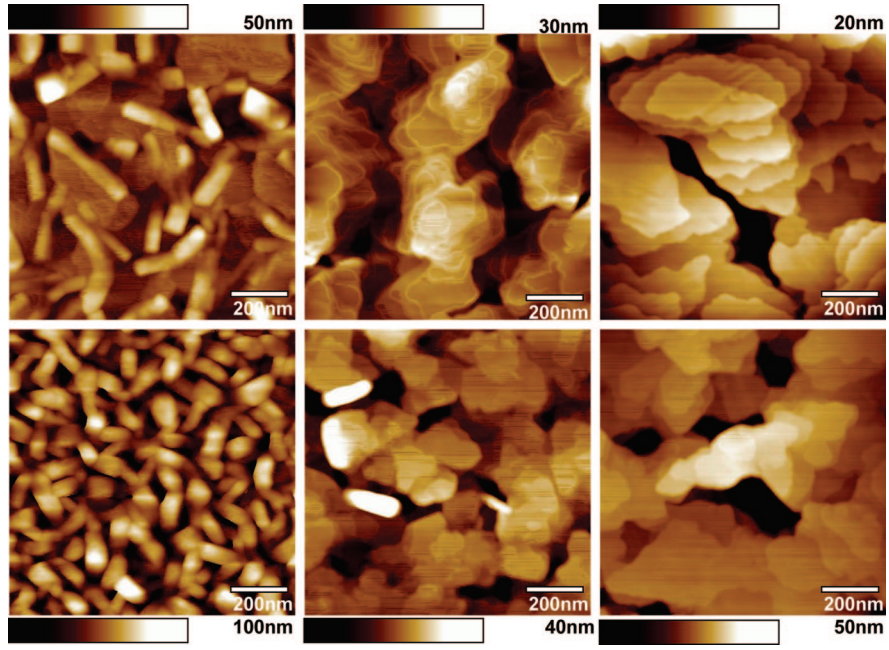

Figure 4. AFM images of **TIPSEthiotetCl$_4$** at a substrate temperate, T_D, of RT (left), 60 °C (middle) and 70 °C (right); on OTS/SiO$_2$/Si (top) and on SiO$_2$/Si (bottom).

Table 3. Summary of the Average OFET Mobilities, μ, and Their Standard Deviations[a]

molecule	T_D/°C		electron (n-) mobilities	hole (p-) mobilities
TIPSEthiotetCl$_4$	RT	μ (cm^2/V s)	0.105 ± 0.01	0.148 ± 0.03
		on/off	9 × 10^5	1 × 10^3
		V_T (V)	+100	+20
	60	μ (cm^2/V s)	0.344 ± 0.06	0.186 ± 0.03
		on/off	1 × 10^5	1 × 10^2
		V_T (V)	+55	+10
	70	μ (cm^2/V s)	0.561 ± 0.1	0.225 ± 0.05
		on/off	1 × 10^5	4 × 10^2
		V_T (V)	+60	+10
TIPSEpentCl$_4$	RT	μ (cm^2/V s)	0.00495 ± 0.001	0.0349 ± 0.002
		on/off	1 × 10^5	9 × 10^4
		V_T (V)	+70	0
	60	μ (cm^2/V s)	0.0537 ± 0.009	0.111 ± 0.003
		on/off	6 × 10^4	5 × 10^3
		V_T (V)	+90	+20
TIPSEpentF$_4$	RT	μ (cm^2/V s)	0.105 ± 0.01	0.0718 ± 0.006
		on/off	2 × 10^5	6 × 10^2
		V_T (V)	+70	+20
	60	μ (cm^2/V s)	0.0782 ± 0.004	0.0325 ± 0.002
		on/off	6 × 10^4	3 × 10^2
		V_T (V)	+70	+20
TIPSEpentF$_8$	RT	μ (cm^2/V s)	0.0335 ± 0.008	0.0964 ± 0.04
		on/off	5 × 10^5	5 × 10^2
		V_T (V)	+25	−5
	60	μ (cm^2/V s)	0.409 ± 0.05	0.330 ± 0.08
		on/off	1 × 10^6	2 × 10^2
		V_T (V)	+50	−15
	80	μ (cm^2/V s)	0.371 ± 0.2	0.269 ± 0.1
		on/off	1 × 10^6	1 × 10^3
		V_T (V)	+50	−15
Cl$_{16}$CuPc	200	μ (cm^2/V s)	0.12 ± 0.01	no hole transport
		on/off	1 × 10^5	
		V_T (V)	+(7−25)	

[a] With the on/off ratio of the source-drain current, "on/off"; and threshold voltages, V_T, on 45 nm top contact devices with gold electrodes on OTS-treated surfaces, $W/L = 20$, $L = 100$ μm, measured in dry nitrogen. The on/off ratio of the source-drain current was calculated as the ratio of the absolute values of the maximum current to the absolute values of the minimum current in a transfer curve. The average reported is the logarithmic average.

counterparts. This red-shift and lower HOMO−LUMO gap is also observed in other conjugated molecules with Cl and F

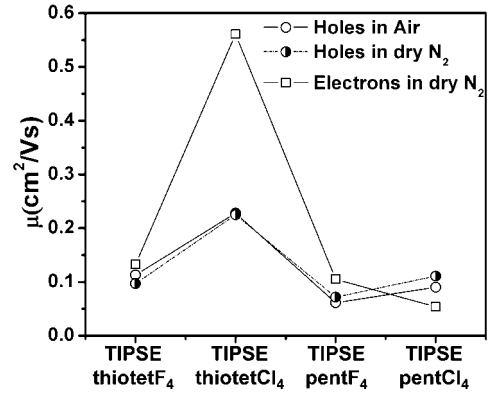

Figure 5. Average mobilities for both holes and electrons in air and in dry nitrogen. No electron transport is observed in ambient. The average mobilities are obtained from the best device conditions, which are RT on OTS for **TIPSEthiotetF$_4$** and **TIPSEpentF$_4$**, 60 °C on OTS for **TIPSEpentCl$_4$** and 70 °C on OTS for **TIPSEthiotetCl$_4$**.

substitutions. For the copper phthalocyanine molecules, due to their poor solubility, only thin film characterization by UPS and UV−vis was performed. **Cl$_{16}$CuPc** has a bandgap of 1.43 eV in thin film and an ionization potential of 5.53 eV (Table 1), whereas **F$_{16}$CuPc** has a bandgap of 1.48 eV (similar to 1.5 eV reported by the Kahn group obtained by X-ray and ultraviolet photoemission spectroscopy[34]) and an ionization potential of 5.65 eV. The UV−vis spectra of 45 nm thin films of both molecules on quartz is in the Supporting Information. Consistent with prior observations,[35] it seems that the ionization potential increases with the fluorination of the CuPcs. The tetrafluorinated acenes have a higher ionization potential of 5.25 eV compared to the 5.13 eV of their tetrachlorinated counterparts.

Thin Film X-ray Diffraction. We performed X-ray diffraction (XRD) on the 45 nm thin films on various surfaces grown under

(34) Shen, C.; Kahn, A. *J. Appl. Phys.* **2001**, *90*, 4549–4554.
(35) Peisert, H.; Knupfer, M.; Schwieger, T.; Fuentes, G. G.; Olligs, D.; Fink, J.; Schmidt, T. *J. Appl. Phys.* **2003**, *93*, 9683–9692.

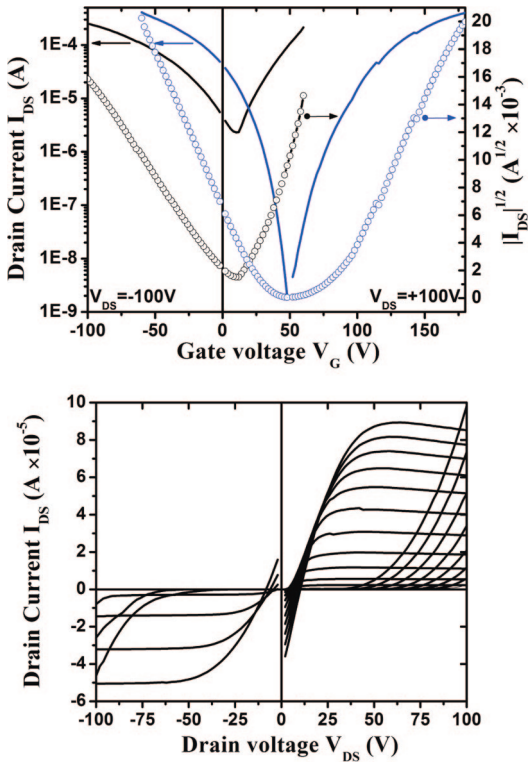

Figure 6. Typical transfer (top) and output (bottom) curves of **TIPSEthiotetCl$_4$**, on OTS-treated SiO_2, for devices grown at a substrate temperature, T_D of 60 °C, $L = 100$ μm, $W/L = 20$. (Top) Solid lines refer to drain current vs gate voltage (*y*-axis on left), while the open circles refer to the square root of the drain current vs gate voltage (*y*-axis on right). (Bottom) For the output curves, the gate voltages ranges from 0 to −100 V (−20 V increments) for holes and from 0 to +180 V (+10 V increments) for electrons.

device conditions. The results are summarized in Table 2, and plots of the XRD data are in the Supporting Information. As can be seen, the chlorinated acenes have a longer out-of-plane *d*-spacing at around 17.3 Å, compared to 16.7−16.8 Å for the fluorinated molecules, and the out-of-plane component of the tetraceno[2,3-*b*]thiophene unit cell close to that of their pentacene analogues. For all these films, the intensity and the full width at half-maximum (fwhm) of the peaks correlate with mobility, with films that have a higher mobility showing more intense and narrower XRD peaks. In comparison, the *d*-spacings of the unhalogenated parent molecules are 16.86 Å for 6,13-TIPS-ethynylpentacene,[36] and 16.4 Å for 5,12-TIPS-ethynyltetraceno[2,3-*b*]thiophene.[37]

Atomic Force Microscopy (AFM). Tapping mode AFM images of the 45 nm thin films made under the same conditions as those used for devices are shown. Figure 3 shows 5 μm × 5 μm images of the two new tetrachlorinated molecules, **TIPSEthiotetCl$_4$** and **TIPSEpentCl$_4$**, as well as the fluorinated pentacene molecules,[27] **TIPSEpentF$_4$** and **TIPSEpentF$_8$** on octadecyltrimethoxysilane (OTS) functionalized SiO_2/Si surfaces that had the best OFET mobilities. Large grains on the order of 2 μm with well-resolved terraces are observed except for **TIPSEpentCl$_4$**. However, all these compounds gave high hole and electron mobilities. This is in contrast with the unhalogenated TIPS-ethynylpentacene[38] and TIPS-ethynyltetraceno[2,3-*b*]thiophene[37] molecules that do not exhibit such terraced thin film character. Molecular terraces on the order of micrometers are also observed on the SiO_2/Si surfaces as can be seen in Figure 4. Figure 4 shows 1 μm × 1 μm AFM images of **TIPSEthiotetCl$_4$** at several substrate deposition temperatures (T_D), and on two types of substrates (OTS/SiO_2/Si and SiO_2/Si). AFM images of the other acenes are in Figures S6−S8 of the Supporting Information. Like most other acenes, these compounds show an increase in grain size with T_D (Figure 4). At T_D = RT, elongated 3D grains at up to twice the deposited thickness of 45 nm (as measured by a quartz crystal monitor during deposition) dominate, but when T_D is increased, large, micrometer-sized molecular terraces are observed. With the exception of **TIPSEpentF$_4$**, the best mobilities are observed when T_D = 60−80 °C, where the largest grain size was observed.

Field-Effect Transistor Characterization. We made devices from the molecules at T_D = RT and 60 °C on 300 nm thermally grown bare SiO_2 and OTS-treated SiO_2. A heavily doped Si substrate served as the common bottom gate electrode. Top-contact/bottom gate transistors were made by evaporating the molecules under high vacuum (10^{-6} torr) to a thickness of 45 nm, as measured by a quartz crystal monitor during deposition. OFETs were measured both in air and in a dry nitrogen glovebox. The mobilities were determined in the saturation regime from the slope of plots of $(I_{DS})^{1/2}$ versus V_{GS}.

Ambipolar behavior was only observed in nitrogen, since the LUMOs of these acenes are still relatively high, compared to other air-stable n-channel semiconductors,[39] and electron carriers are trapped by ambient species, such as oxygen and moisture.[40] No n-type behavior was observed on bare SiO_2, due to trapping by the silanol groups on the surface of the substrate.[41] Hole currents measured in air did not change for all the molecules (see Table S1, Supporting Information, and Figure 4). For **TIPSEpentF$_8$**, the p-channel threshold voltage surprisingly became more positive in air, leading to lower calculated mobilities. In general, except for **TIPSEpentF$_4$**, both p- and n-mobilities increased with T_D. Both **TIPSEthiotetCl$_4$** and **TIPSEpentF$_8$** showed high and balanced ambipolar OFET mobilities, with the maximum hole mobility and electron mobility of 0.272 cm^2/V s and 0.686 cm^2/V s, respectively, for the former and 0.511 cm^2/V s (holes) and 0.456 cm^2/V s (electrons) for the latter. The asymmetric TIPS-acetylenepentacenes have high mobility for one charge carrier >0.1 cm^2/V s, but a mobility an order of magnitude lower for the opposite charge carrier. Table 3 lists the key OFET characteristics of the acenes and **Cl$_{16}$CuPc** measured in nitrogen, while the Supporting Information includes OFET data obtained in air. Figure 5 plots the average hole and electron mobilities for the best conditions for the acenes both in nitrogen and in air. As can be seen, hole mobility remains the same whether in air or in nitrogen, implying that ambient species do not trap the holes in the acenes. **Cl$_{16}$CuPc** is an air-stable n-type OSC, as previously reported,[23] and the OFET characteristics are the same

(36) Maliakal, A.; Raghavachari, K.; Katz, H.; Chandross, E.; Siegrist, T. *Chem. Mater.* **2004**, *16*, 4980–4986.
(37) Tang, M. L.; Reichardt, A. D.; Siegrist, T.; Mannsfeld, S. C. B.; Bao, Z. N. *Chem. Mater.* **2008**, *20*, 4669–4676.
(38) Sheraw, C. D.; Jackson, T. N.; Eaton, D. L.; Anthony, J. E. *Adv. Mater.* **2003**, *15*, 2009–2011.
(39) Wang, Z.; Kim, C.; Facchetti, A.; Marks, T. J. *J. Am. Chem. Soc.* **2007**, *129*, 13362–13363.
(40) Weitz, R. T.; Amsharov, K.; Zschieschang, U.; Villas, E. B.; Goswami, D. K.; Burghard, M.; Dosch, H.; Jansen, M.; Kern, K.; Klauk, H. *J. Am. Chem. Soc.* **2008**, *130*, 4637–4645.
(41) Chua, L. L.; Zaumseil, J.; Chang, J. F.; Ou, E. C. W.; Ho, P. K. H.; Sirringhaus, H.; Friend, R. H. *Nature* **2005**, *434*, 194–199.

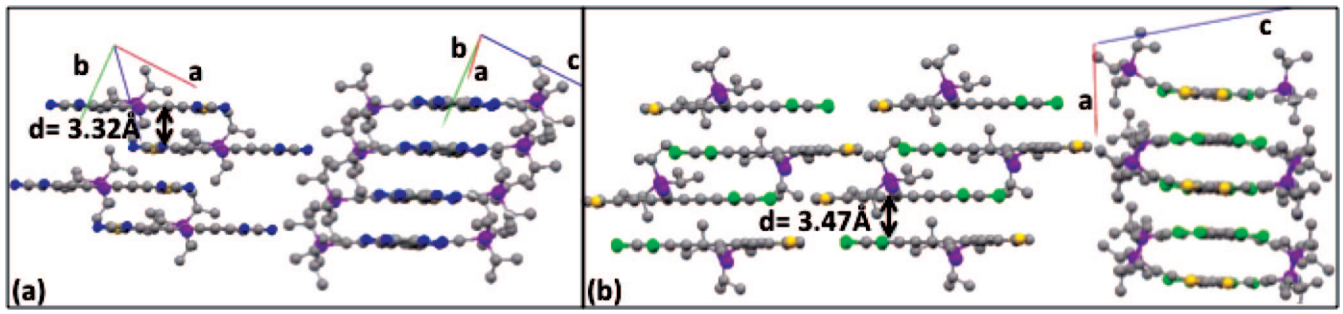

Figure 7. Single-crystal structures of (a) **TIPSEthiotetF$_4$** and (b) **TIPSEthiotetCl$_4$**, with F atoms in blue, Cl atoms in green, S in yellow, Si in purple, and C in gray. On the left of both (a) and (b), looking down the *c*-axis of the unit cell, the TIPS groups are in and out of the plane (The TIPS groups in front have been removed for clarity); on the right of both (a) and (b): the acene backbone perpendicular to the plane, with the TIPS-acetylene groups in plane.

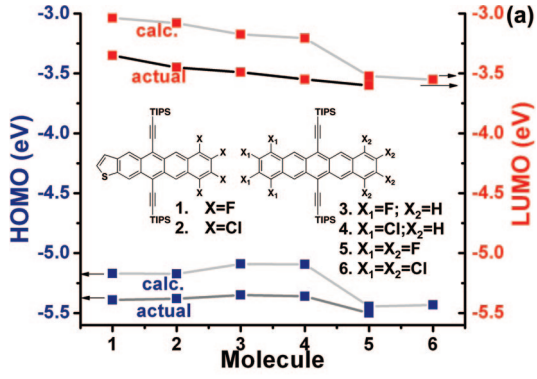

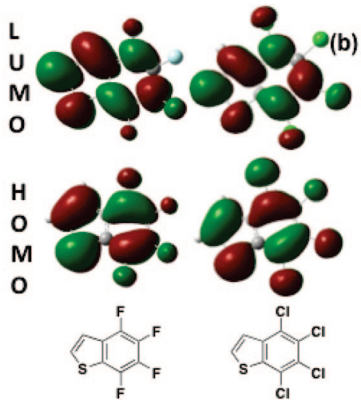

Figure 8. (a) Plot of the measured HOMO and LUMO levels for **TIPSEthiotetF$_4$**, **TIPSEthiotetCl$_4$**, **TIPSEpentF$_4$**, **TIPSEpentCl$_4$**, and **TIPSEpentF$_8$**, and the DFT (B3LYP/6-31G+d) calculated HOMOs and LUMOs, including **TIPSEpentCl$_8$**. (b) MO diagrams for 4,5,6,7-tetrafluorobenzo[*b*]thiophene and 4,5,6,7-tetrachlorobenzo[*b*]thiophene obtained by B3LYP/6-31G+d DFT calculations that show an increased electron density on Cl compared to F for both the HOMO and LUMO.

whether in ambient or in nitrogen, with electron mobility 0.11 cm^2/V s (slightly higher than previously reported, ~0.01 cm^2/V s) over many devices when deposited at T_D = 200 °C on OTS-treated surfaces. Transfer and output curves characteristic of **TIPSEthiotetCl$_4$** are shown in Figure 6, while those from the other molecules are in the Supporting Information.

The acenes discussed here have high and balanced ambipolar transport. This may be partially related to their packing in the single crystal form. The 2D π-stacked single crystal structure enforced by the relatively bulky TIPS groups has been shown for **TIPSEpentF$_4$**, **TIPSEpentF$_8$**[27] and **TIPSEthiotetF$_4$**.[28] **TIPSEthiotetCl$_4$** displays similar kind of packing, as shown in Figure 7a, with the distance between the π-stacks of adjacent molecules being 3.47 Å, compared to 3.32 Å in **TIPSEthiotetF$_4$**.

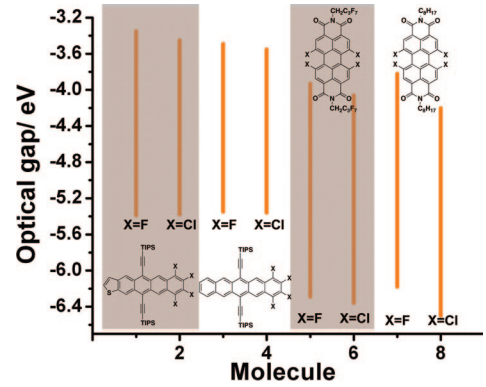

Figure 9. Optical bandgap of the tetrahalogenated molecules in soltution: the acenes in THF and the PDI molecules in CH_2Cl_2. The odd-numbered molecules are tetraflourinated, while the even-numbered molecules are tetrachlorinated. The optical gap is smaller for the chlorinated molecules.

The balanced mobilities may be due to the HOMO and LUMO residing on the same molecular backbone (Figure S13 in the Supporting Information); hence, the transfer integral[42] (a parameter which quantifies the degree of wave function overlap) of the holes and electrons are roughly equal in magnitude. In contrast to **TIPSEthiotetF$_4$** where neighboring acene cores above and below each other are slightly offset with respect to their short axis along the conjugated core, **TIPSEthiotetCl$_4$** has the acene backbone of adjacent molecules packed almost directly above and below each other, with the TIPS-acetylene groups buckling upward or downward due to steric hindrance (Figure 7b). The tetrachlorinated molecule overlaps more with one member of the pair of molecules above and below (Figure 7b), instead of being in between both, as observed in **TIPSEpent** and **TIPSEthiotetF$_4$** (Figure 7a). Unfortunately we did not manage to obtain the single-crystal structure of **TIPSEpentCl$_4$**.

Discussion

The red-shift of the tetrachlorinated acenes by 15−16 nm with respect to their tetrafluorinated and unsubstituted counterparts is qualitatively predicted by DFT calculations (Figure 8a). The HOMOs did not show a significant difference both experimentally and theoretically between the Cl and F molecules, perhaps because these molecules are so large that other parts of the molecule have more significant effect than the four electron-withdrawing halogens on the overall HOMO level. The lower HOMO−LUMO gap in the chlorinated molecules may

(42) Coropceanu, V.; Cornil, J.; da Silva, D. A.; Olivier, Y.; Silbey, R.; Bredas, J. L. *Chem. Rev.* **2007**, *107*, 926–952.

be thought of in terms of an increase in delocalization. Using benzo[*b*]thiophene as a test system for our molecules, with the B3LYP level of theory and a 6-31 g+d basis set, the same red-shift is predicted for the tetrachlorinated molecule over its tetrafluorinated counterpart. The MO diagrams reveal that for both the HOMO and LUMO, there is increased electron density over the chlorine atoms compared to the fluorine atoms (Figure 8b). This may be due to the electron-withdrawing nature of halogens. Cl has empty 3d orbitals to accommodate any delocalization of the π-electrons, but the 3s being the next unoccupied atomic orbitals on F, are prohibitively high in energy. Furthermore, the small radii characteristic of F would result in severe electrostatic repulsion if the π-electrons were to delocalize in its vicinity. Figure 8b shows the results of the B3LYP/6-31 g+d calculations for benzo[*b*]thiophene.

Others have also calculated this red-shift from F to Cl for **PDI**-based molecules functionalized in the bay positions with two halogens (**PDIF$_2$** and **PDICl$_2$** in Figure 1), using both DFT and TDDFT, which can more accurately reproduce experimental results.[36] They attribute the decrease in the HOMO−LUMO gap from 2.50 eV to 2.44 eV[43] from **PDIF$_2$** to**PDICl$_2$** (by TDDFT) to the halogen p orbitals contributing to the wave function belonging to the HOMO for Cl, Br, and I, but less for F, such that the increased delocalization of the electrons in the HOMO reduces the HOMO−LUMO gap. Experimentally, we can compare the λ_{abs} in dichloromethane of the tetrahalogenated **PDI**s reported by the Würthner and Marks groups. In dichloromethane, **PDI-FF$_4$** has a λ_{abs} (the long wavelength absorption maxima) of of 502 nm,[14] while **PDI-FCl$_4$** has a λ_{abs} of 519 nm,[21] a red-shift of 17 nm. A red-shift of 14 nm is observed from **PDI-8F$_4$**[32] to **PDI-8Cl$_4$**.[21] Figure 9 summarizes the optical gaps of tetrahalogenated molecules in solution from this work and published reports.[21,32] Since the HOMOs between chlorinated and fluorinated molecules show little difference, the smaller HOMO−LUMO gap for the chlorinated molecule results in a lower LUMO.

Cl$_{16}$CuPc has an electron mobility of 0.11 cm^2/V s in air at T_D = 200 °C on OTS which is an order of magnitude higher than the 0.03 cm^2/V s[44] reported for **F$_{16}$CuPc** on SiO_2. For the acenes, **TIPSEthiotetCl$_4$** has higher ambipolar mobilities than **TIPSEthiotetF$_4$**, while **TIPSEpentCl$_4$** and **TIPSEpentF$_4$** have the same performance as OFETs. This trend of chlorinated molecules performing as well as the fluorinated ones extends further to PDI-based OSCs. While unfunctionalized **PDI** (Figure 1) is not an air-stable n-type OFET, **PDI-Cl$_4$** has an electron mobility of 0.1 cm^2/V s[24] in air on OTS-treated surfaces, comparing well with **PDI-FF$_2$** and **PDI-FF$_4$**[14] which have a mobility of 0.34 cm^2/V s and 0.03 cm^2/V s respectively. Prior to characterization as an OFET, **PDI-Cl$_4$** has been shown to transport electrons[25,45] by pulse radiolysis time-resolved microwave conductivity (PR-TRMC). However, not all chlorinated PDIs work well; **PDI-FCl$_4$**[21] has very low mobility and is blue-shifted in solution compared to the parent molecule unhalogenated at the bay positions, presumably due to the distortion of the PDI core induced by the steric demands of four chlorine atoms in the bay positions. While **PDI-Cl$_4$** has the same distortion of the PDI core as that of **PDI-FCl$_4$**, its higher high mobility may be attributed to morphological factors.

Conclusion

We have shown that chlorination is a viable route to n-type OFETs by synthesizing chlorinated acenes, characterizing chlorinated **CuPc**, and drawing on examples in literature from the **PDI** family. Chlorination appears to be a general route toward electron transporting OSCs that has so far not been intensively explored as fluorination has. We show that chlorinated molecules behave as well or better than their fluorinated counterparts in terms of electron mobility and ambient stability. If chlorine atoms are introduced in such a way as not to distort the planarity of the conjugated core, chlorinated molecules typically have a lower LUMO than their fluorinated counterparts due to delocalization of π-electrons into the unoccupied 3d orbitals that are not available in F. This is advantageous in terms of electron injection as the Schottky barrier is decreased, and makes the charge carriers in the active layer less susceptible to trapping by oxygen and moisture. Chlorination is a way to fine-tune the level of the LUMO in organic semiconductors. In light of the fact that chlorinated precursors are more easily available and cost less than fluorinated ones, this observation introduces new avenues in the design of organic semiconductors.

Acknowledgment. We thank Prof. John I. Brauman and Prof. Christopher E. D. Chidsey for valuable discussions. M.L.T. acknowledges a Kodak graduate fellowship, J.H.O. partial financial support from the Korea Research Foundation Grant (MOEHRD KRF-2006-352-D00066) and A.D.R. a Major grant from Stanford. Z.B. acknowledges partial financial support from the Global Climate and Energy Project (GCEP) and an AFSOR Grant.

Supporting Information Available: Supporting Information with the detailed synthetic procedures, out-of-plane XRD plots, AFM images, OTFT transfer and output curves, molecular modeling coordinates, molecular orbital diagrams, UV−vis of **Cl$_{16}$CuPc** and **F$_{16}$CuPc** and the crystallographic information file (CIF). This material is available free of charge via the Internet at http://pubs.acs.org.

JA809045S

(43) Mete, E.; Uner, D.; Cakmak, M.; Gulseren, O.; Ellialtoglu, S. *J. Phys. Chem. C* **2007**, *111*, 7539–7547.
(44) Bao, Z. A.; Lovinger, A. J.; Brown, J. *J. Am. Chem. Soc.* **1998**, *120*, 207–208.
(45) Graaf, H.; Michaelis, W.; Schnurpfeil, G.; Jaeger, N.; Schlettwein, D. *Org. Electron.* **2004**, *5*, 237–249.